Journal of Building Engineering 57 (2022) 104825

Contents lists available at ScienceDirect

Journal of Building Engineering

journal homepage: www.elsevier.com/locate/jobe

Semi-dry technology mediated lignocellulosic coconut and energy reed straw reinforced cementitious insulation panels

Zsuzsanna Mária Mucsi [a,*], K.M. Faridul Hasan [a], Péter György Horváth [a,**], Miklós Bak [a], Zsófia Kóczán [a,b], Tibor Alpár [a,***]

[a] Faculty of Wood Engineering and Creative Industries, University of Sopron, Sopron, 9400, Hungary
[b] Paper Research Institute, University of Sopron, Sopron, 9400, Hungary

ARTICLE INFO

Keywords:
Lignocellulosic materials
Coir and reed straw
Sustainable building materials
Semi-dry technology
Cementitious panel

ABSTRACT

Sustainable cementitious composite panels are gaining interest as efforts to reduce environmental burdens increase. This study investigated the possibilities and reinforcement effects of developing composite panels from coconut husk derived materials (CM) and reed straw (RS) particles in the presence of Ordinary Portland cement (OPC). Five composite panels with 1200 kg/m^3 densities and 400 × 400 × 8 mm^3 dimensions were produced. The proportion of lignocellulosic materials for energy reed and coconuts were 100:0, 60:40, 50:50, 40:60 and 0:100%, respectively. Other ingredients like OPC, Na_2SiO_3, and cement stone were kept constant. The panels were produced by utilizing energy efficient semi-dry technology, a novel fabrication technology that requires less water to make the slurry. The investigations – thermal conductivity, mechanical, physical, FTIR (Fourier transform infrared spectroscopy) and morphological – were conducted after 28 days of curation in a standard laboratory atmosphere. The test obtained the following results: the thermal properties of cementitious coconut and reed panels show that the thermal conductivity of the mixture expresses the excellent insulating properties of the panels. The thermal conductivity coefficient ranged from 0.11 to 0.15 W/(mK), with reed-only boards attaining superior values. Mechanical properties such as flexural strength and internal bonding strength showed an increasing trend as the amount of coconut increased. The panel containing coconut materials only achieved the best values – 5.13 MPa (flexural strength) and 0.31 MPa (internal bonding strength). The morphological images displayed the presence of lignocellulosic materials in the composite structures, whereas the FTIR study provides evidence of successful chemical interactions between the OPC and reinforcements. The results reveal a novel, eco-friendly and green composite panel fabrication technology that can facilitate panel manufacturers, especially in the construction and building sectors.

1. Introduction

The push towards environmental sustainability has increased interest in naturally derived lignocellulosic materials. Although human beings have been using these naturally-originated materials for millennia, their use has been limited in recent decades due to

* Corresponding author. 9400, Bajcsy-Zsilinszky u. 4., Sopron, Hungary.
** Corresponding author.
*** Corresponding author.
E-mail addresses: zsuzsi.mucsi@gmail.com (Z.M. Mucsi), horvath.peter.gyorgy@uni-sopron.hu (P.G. Horváth), alpar.tibor@uni-sopron.hu (T. Alpár).

https://doi.org/10.1016/j.jobe.2022.104825
Received 8 March 2022; Received in revised form 23 May 2022; Accepted 14 June 2022
Available online 20 June 2022

the lack of feasible technological progress. Nevertheless, these materials are being rediscovered today for the following reasons: their eco- and environment-friendly properties, their abundance (e.g. as by-products), new technologies that provide new processing opportunities, and the growing interest in using naturally derived materials instead of concrete or plastics [1–5]. Natural derived cellulosic materials show significant potentiality in optimizing reinforcement architecture. The new technologies offer the opportunity to use these ancient materials in the most advanced way and allow for the environmentally friendly recovery of increasing amounts of waste and by-products [6–8]. The present study focuses on coconut particles and common reed straw material. The combination of these materials helps provide possible solutions to global and local building materials sustainability problems. Both natural materials have excellent properties (less sensitive to moisture, good strength values, mould and fungus resistance, etc.). Their combination is promising, but also raises problems, e.g. finding the right mix ratio [9–12].

Generally, lignocellulosic biomass materials are tightly packed with cellulose, lignin, and hemicellulose matrix in their polymeric structures [13–17]. Moreover, they are also environmentally friendly and renewable sources to produce sustainable products [18–22]. Researchers have previously developed some composites using natural coconut and/or reed materials for applications like thermal insulation and acoustic panels [23–25]. This investigation deals with lightweight construction material production technology. Coconut fibres/particles have been often used in lightweight cement-based products. In many cases, they are pre-prepared and are often washed or boiled, but in other cases, the raw materials are directly used without any treatments. These cement-bonded coir boards showed lower thermal conductivity than commercial flakeboard composites in several cases, and the produced boards also satisfy most recommended mechanical standards [26,27]. Cellulosic reed materials possess great potential as feedstock for concrete materials. Some important factors to consider are reed origin, soil composition, and harvest time [10,28,29]. Researchers are increasingly interested in developing hybrid composites that mix two different cellulosic materials (different proportions) for improved thermo-mechanical performances [16,30–34]. However, the possibility of hybrid composites developed from coir and reed straw in the presence of an OPC matrix has not yet been reported.

Cement, especially OPC, is a widely used binder in the construction industry; however, producing cement is an energy-intensive process. Cement is an artificially produced, finely-ground inorganic binder. When mixed with water, it solidifies both in air and in water. Its raw material is limestone, clay, and marl. These materials are mixed in appropriate proportions, burned and then finely ground. Portland cement is obtained by adding gypsum powder to this clinker. In addition, cement main contains other additives. Portland cement consists of four main clinker materials: alite (tricalcium silicate, $Ca_3O \cdot SiO_4$), belit (dicalcium silicate, Ca_2SiO_4), felit (tricalcium aluminate, $3CaO \cdot Al_2O_3$), and celit (tetracalcium aluminate ferrite, $4CaO \cdot Al_2O_3Fe_2O_3$) [35,36]. The cement-bonded natural fibre-based composites have feasible characteristics; however, the types of cement are not easily compatible with the fibres because of the presence of some inhibitory materials such as tannin, sugar, starch, phenols, hydroxylated carboxylic acid and others [37–39].

Organic cellulosic materials can be used as reinforcement either in cement matrix or polymer composites. The two types of lignocellulosic materials bound with cement affect many properties of the lightweight boards in different ways, and cement is a more traditional binder than other types of polymers. For these reasons, the current investigation uses OPC as a binder. The prime objectives were used to determine and compare the physical, mechanical and thermal properties of the composite boards. The boards were measured according to relevant standards. This paper has studied their performance as discontinuous and randomly distributed lignocellulosic materials in a cementitious matrix of thin prefabricated panels as a good substitute for conventional materials, both to improve mechanical performance and increase thermal insulation properties. Scanning electron microscopy (SEM) images were used to check the arrangement of natural fibres and cement in the composite system. Moreover, the novel semi-dry technology used to fabricate the panels has not yet been reported for hybrid cementitious panel production from CM and RS materials. Traditionally, fibre/wood cement panels are made using Hatchek/wet processing technology [40,41]; however, a semi-dry technology is implemented for this current study to minimize water and associated energy consumption. To date, semi-dry technology is popular for the wood particle reinforced cement-bonded panels [42], whereas this method is not yet widely studied for cellulosic materials like reeds straw/coconut husk-based particles/cement panels.

2. Materials and methods

2.1. Materials

The coconut materials used in this study were extracted from coconut husks covering the fruit of a coconut palm (*Cocos nucifera* L.). We obtained big brown particles from a Hungarian company Pro Horto Ltd. (Szentes, Hungary). They were crushed into smaller particles and sieved before fabrication into composites. The size of the sieved particles were 0–6 mm. Typical coconut materials contain nearly 36–43% cellulose, 10–20% hemicellulose, 41–45% lignin, and 3–4% pectin [43]. The coconut materials came from India. The reed straws were provided by another local company, VNÁD Nádipari Kft., and it was harvested near Lake Fertő, Hungary. Commercially used Ordinary Portland Cement (manufactured by Duna-Dráva cement Kft. Vác, Hungary) was supplied by FALCO Woodworking Co., Hungary. The main constituents of OPC are CaO (64.49%), SiO_2 (19.01%), Al_2O_3 (5.51%), Fe_2O_3 (3.81%), MgO (0.43%), Na_2O (0.28%), TiO_2 (0.27%), Cl (0.01%), and loss in ignition (2.34%) [44]. The additive (Na_2SiO_3) used for producing the panels was procured from Sigma Aldrich (Hungary).

2.2. Methods

2.2.1. Preparation of reed and fibrous coir chips

We crushed the coconut chips and reed straws into smaller pieces using VZ23412 model grinding equipment (Dynamo Budapest located in Hungary) to create the smaller particles. We then sieved the ground particles with a sieve analyser (ANALYSETTE 3PRO, Fritsch, Germany) within a range of dimensions to understand the particle dimensions. The amount remaining on each sieve plate was

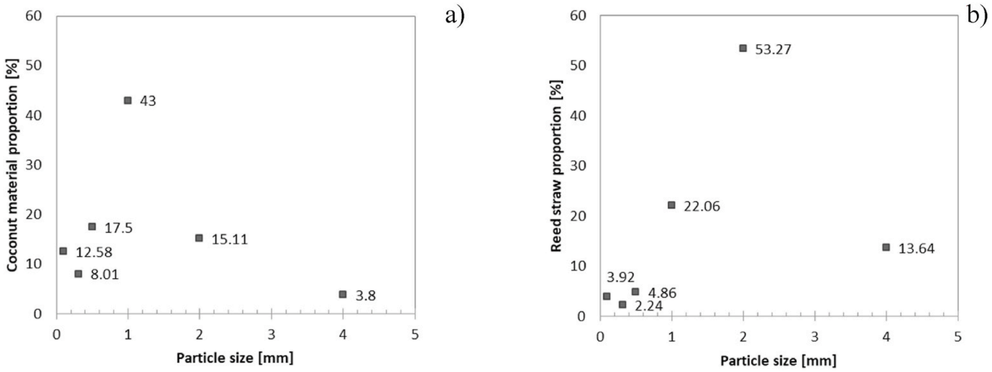

Fig. 1. Size distribution of lignocellulosic materials: (a) coir and (b) reed material.

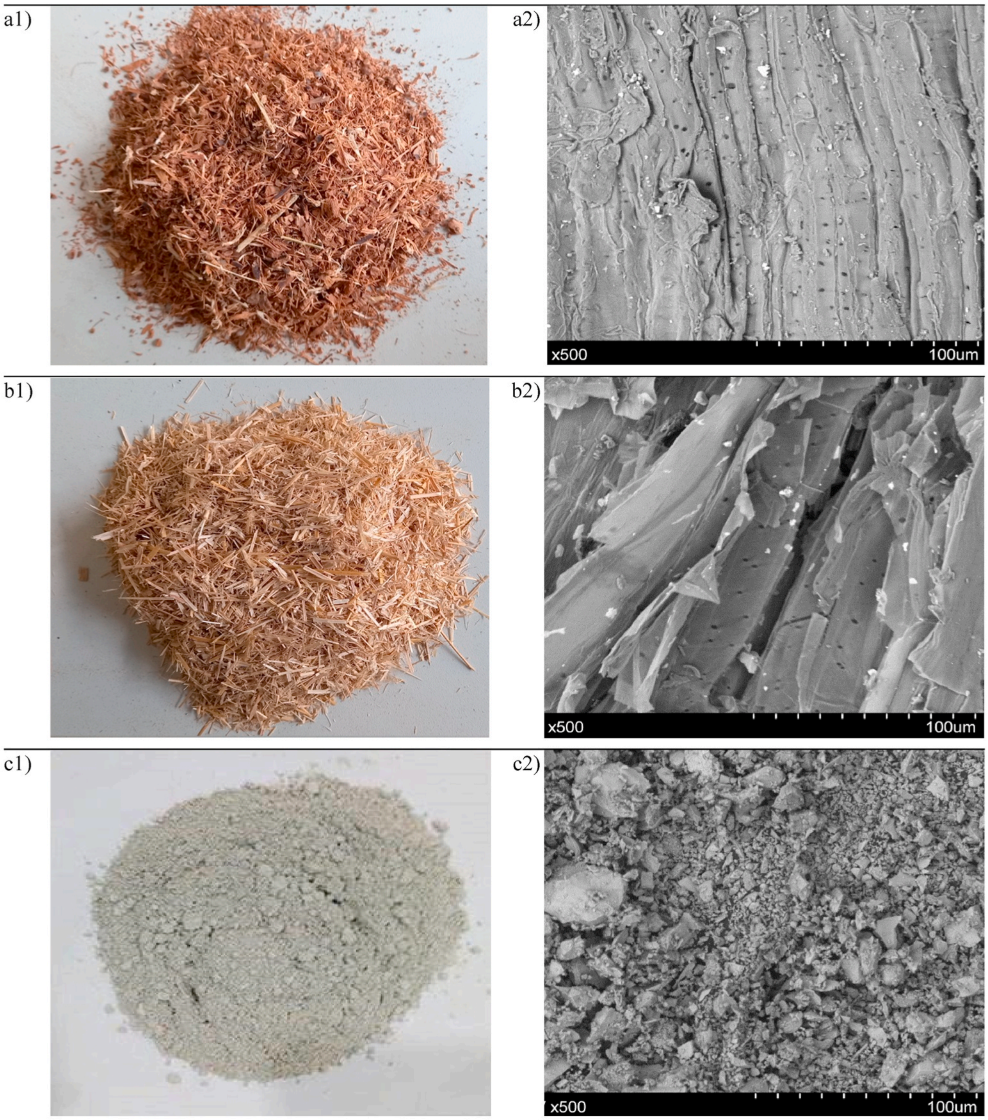

Fig. 2. Physical and morphological photographs of coir particles, reed particles, and OPC material. (a1) Physical photographs of coir material; (a2) SEM image of coir material; (b1) Physical photographs of reed material; (b2) SEM images of reed material; (c1) Physical photographs of OPC; (c2) SEM image of OPC.

Table 1
Recipe for OPC bonded coir/reed material products, OPC– Ordinary Portland cement; Na_2SiO_3–Water glass (proportions).

Materials/chemicals	CEM1	CEM2	CEM3	CEM4	CEM5
Reed straw	1.00	0.60	0.50	0.40	0.00
Coir	0.00	0.40	0.50	0.60	1.00
OPC	2.6	2.6	2.6	2.6	2.6
Na_2SiO_3	0.052	0.052	0.052	0.052	0.052
Cement Stone	0.52	0.52	0.52	0.52	0.52

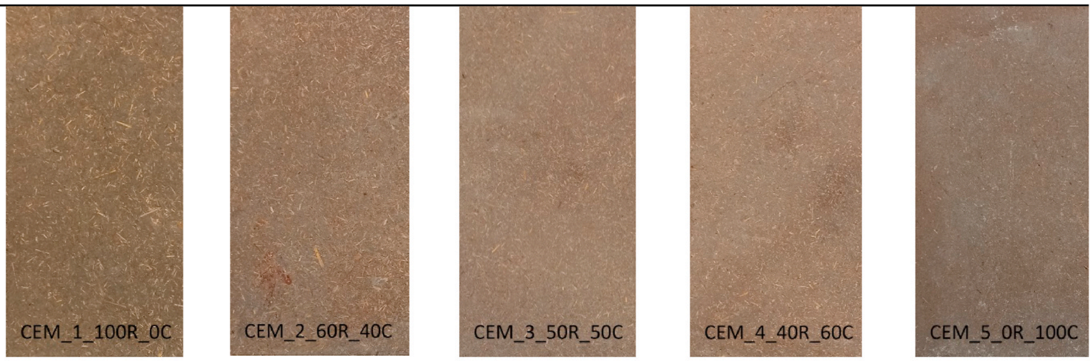

Fig. 3. Physical photographs of produced composite panels from coir and reed material with OPC (CEM1– CEM5).

measured as a percentage. The sizes of the sieves were 0.315, 0.5, 1.0, 2.0 and 4.0. The obtained dimension for coconut and reeds particles were within 0–6 mm. The maximum portions of reed straws were within 2 mm and coir particles within 1 mm (Fig. 1). To ensure the moisture contents of the lignocellulosic materials were within a tolerable range, we assessed the moisture contents of the coconut and reed straws according to the EN 322:1993 standard before fabrication. However, a standard accuracy was maintained during these testing protocols (0.001 g at 105 ± 0.3 °C). The moisture contents of coir and reed particles were 5.40% and 8.10%, respectively.

2.2.2. Characterization of materials

Physical and SEM morphographs were taken (Fig. 2). We used the SEM images – taken with a Hitachi S–3400 N instrument (Japan) at an accelerating voltage of 20.0 kV for particle boards and 20.0 kV for fractured composites – to observe the structure and defects of the produced composite panels. The reed surface is smooth and evenly long-grooved, while the coconut surface is rough and uneven in the photographs. The shape of the cement grains is grooved with irregular edges and a rough surface.

2.2.3. Composite panel production

The recipe for reed straw and coir particle reinforced cementitious materials is presented here in proportion as used for recipe formulation (Table 1).

We produced five boards with 400 × 400 × 10 mm3 dimensions using semi-dry technology (Fig. 3). The first board contained 100% reed and 0% coconut particles (CEM1). The second was 60% reed and 40% coconut particles (CEM2). The third board contained 50% reed and 50% coconut particles (CEM3). The ratio of the fourth board was 40% reed and 60% coconut particles (CEM4), and the fifth board was 0% reed and 100% coconut particles (CEM5). The panel production ratio of lignocellulose to cement in cementitious composites in industrial production is about 1: 2.6. The binder is OPC and the additives are water and water-glass, in the same quantity for each table. Cementitious composites form a spreadable mixture with a moisture content of 40% to ensure proper cement bonding. We used as much water as possible to reach this 40% value, which resulted in 42% water per panel used during operation. We prepared the slurry by mixing the ingredients in the recipe (Table 1). Initially, we placed the lignocellulosic materials and OPC into a drum and mixed them properly and continuously with an electric stirrer. Later, we dripped the mixed water and water glass solution into the drum as we continued stirring. Once the slurry formed, we placed it in the moulded wooden frames (400 × 400 mm^2) over a steel plate and pre-pressed it with another wooden lid. The pre-pressed mat was covered with a polybag and placed in the pressing machine. Every panel is 10 mm thick and has a nominal density of 1200 kg/m^3. The compression moulding machine pressed the plates at a pressure of 7.2 MPa. The temperature of the plates was 23 °C, and the pressing lasted 24 h. After compression, the composite panels were cured at close to room temperature (25 °C) and 65% relative humidity for another 28 days. After the panels solidified, we cut them according to a particular size.

2.2.4. Characterization of the developed products

Initially, we tested the wax of the reed and coconut materials with a laboratory-based analytical method. Moreover, we performed moisture content analysis on the reed and coir particles according to the EN 322:1993 standard using a moisture analyser (Kern ULB 50-3 N, KERN AND SOHN GmbH Co., Germany) before producing the panels. Panel surfaces should be smooth and uniform. The

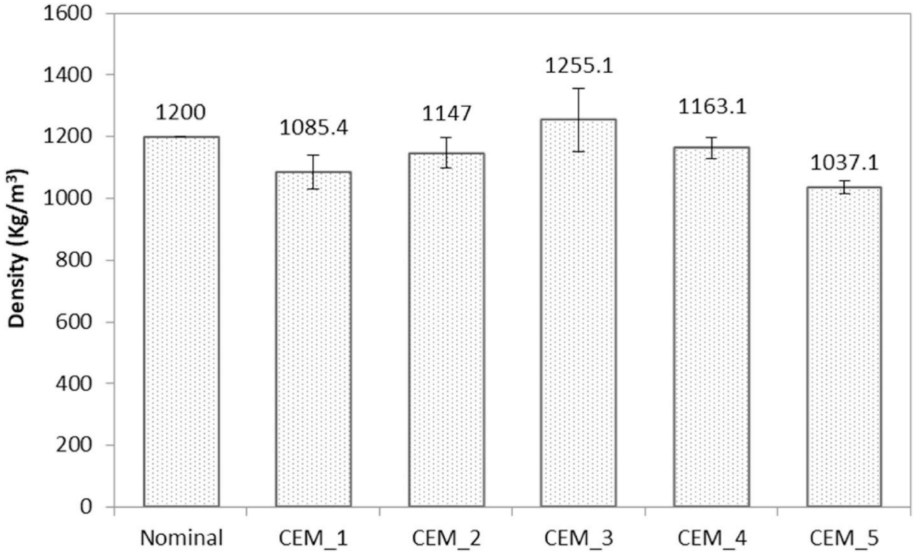

Fig. 4. Nominal and actual densities of the produced composite boards.

detailed description of this test was discussed in our previous study for different cellulosic material reinforced cementitious composites [31]. We measured the mechanical properties of the cementitious panels with an Instron testing machine (4208, USA), and we adopted standards EN 310 for flexural properties tests and EN 319 for internal bonding strengths tests. The crosshead movement speeds during the tests were 0.8 and 5.0 mm/min, respectively for flexural internal bonding strengths characterizations. Morphological images were captured by SEM testing equipment (S3400 N, Hitachi, Japan) at 15.0 kV. We conducted TGA and DTG tests using a TGA instrument (Themys thermal analyser, Setaram Instrumentation, France) at 10 °C/min ranging from 50 to 850 °C under a nitrogen atmosphere. FTIR studies were performed within 4000 to 400 cm^{-1} using an FTIR-6300 model instrument – produced by the Japanese company Jasco – to assess the chemical bonding between OPC and lignocellulosic materials. Additionally, we determined the water absorption, thickness swelling, and moisture contents of the samples according to the MSZ 1336:4–13379, EN 317, and EN 322 standards, respectively.

For the flexural tests, the sample dimensions were 290 × 50 mm^2. The load was applied perpendicularly at the centre of the samples by maintaining a constant speed until the breakage occurred. The internal bonding strength of the boards was also measured using the same Instron machine but with a different design as per standard 50 × 50 mm^2. The testing speed for flexural properties was 0.8 mm/min and 5.0 mm/min for internal bonding strength. The modulus of rupture for the cement composite board was calculated based on Equation (1), and the modulus of elasticity is calculated as per Equation (2).

$$\text{Modulus of rupture} = \frac{3}{2}\frac{\boldsymbol{Fl}}{\boldsymbol{bt^2}} \qquad \text{Equation 1}$$

Where F = maximum force/load in N, L = span length in mm, b = width of specimens in mm, t = thickness of specimens in mm, a = deflection.

$$\text{Modulus of elasticity; Em} = \frac{l_1^3 \times (F_2 - F_1)}{4 \times b \times t^3 \times (a_2 - a_1)} s \qquad \text{Equation 2}$$

Where l_1 = span of support [mm], b = width of specimen [mm], t = thickness of specimen [mm], F_2–F_1 = increase of load in N on the straight section of the load– deflection curve. F_1 at 10% of (F_{max}), F_2 at 40% of (F_{max}), a_2–a_1 = increase of deflection of the test pieces measured at the centre of the test sample in connection with the increase in load.

In the water absorbency (WA) and thickness swelling (TS) tests, the sample dimensions were 50 × 50 mm^2. We weighed the samples with an electric balance (Bizerba, SL– 2100 M, Italy) and measured thicknesses using Mitutoyo 543-551D equipment (Mitutoyo Europe GmbH, Neuss, Germany). We placed all the samples into water for 2 h and then measured the weight and thickness values afterwards. Once we had completed these measurements, we immersed the pieces into the water again for another 22 h (altogether 24 h). Finally, we measured water absorbance (Equation (3)) and thickness swelling (Equation (4)) once more using Equation (4) was used to calculate the water absorbency of the samples and Equation 5 for thickness swelling measurements. The duration (t) was the same in both studies, at 2-h and 24-h intervals.

$$\text{Water absorbance (time)} = \frac{\boldsymbol{W_w} - \boldsymbol{W_d}}{\boldsymbol{W_d}} \times 100 \qquad \text{Equation 3}$$

Where W_w is the weight of wet sample, W_d is the weight of dry samples.

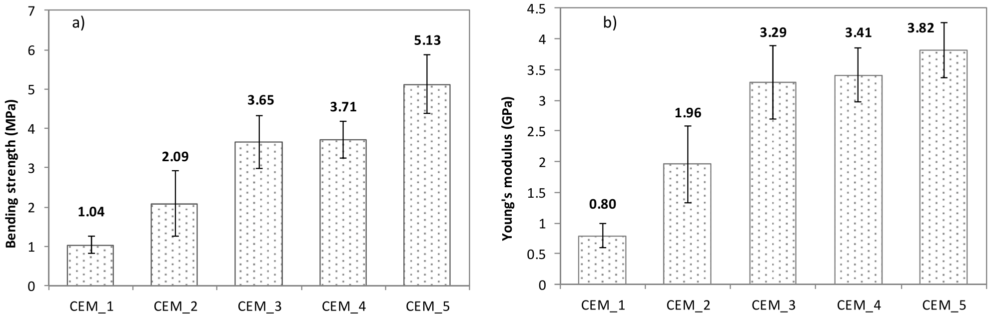

Fig. 5. Flexural characteristics of composites: a) Bending strength and b) Young's modulus.

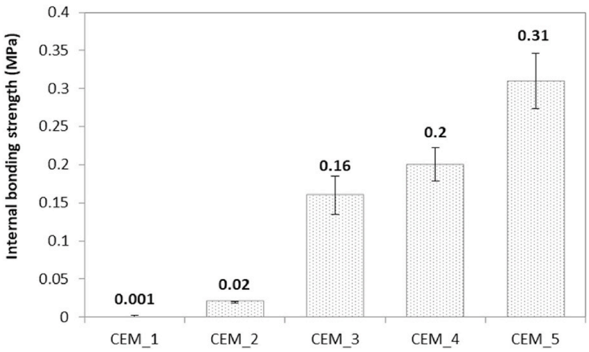

Fig. 6. Internal bonding strength of composites.

$$\text{Water absorbance (time)} = \frac{T_w - T_d}{T_d} \times 100 \quad \text{Equation 4}$$

Where T_w is the thickness of the wet sample, T_d is the thickness of the dry samples.

3. Results and discussion

3.1. Wax content tests

We tested the wax content of the control coconut materials and reeds straw particles. The ground cane sample was sieved and 3 g of cyclohexane (100 mL) was extracted in Soxhlet for 24 h. This solvent extracts the resin materials. Then, 20 mL of the resulting solution was evaporated to dryness, and the residual weight was measured to be about zero. Consequently, reed wax content is negligible. This is very important because of the connection between the lignocellulosic particles and the cement grains; the presence of wax weakens the connection between the raw materials.

3.2. Mechanical properties

We considered the nominal density of the panels to be 1200 kg/m^3 before the recipe formulation and composites fabrications. The actual densities of each composite were as follows: 1085.38; 1146.98; 1255.13; 1163.05, and 1037.08 kg/m^3, respectively (Fig. 4). The density values were lower in four of the five panels, and for one board, it was more than the design value. In three cases, the difference was insignificant (CEM2, CEM3, CEM4), but it was higher in the other two cases (CEM1, CEM5). However, this unevenness did not cause much variation in the test results. The discrepancies likely arose because we produced the boards manually, which made proper homogeneity difficult to achieve. In addition, we also created and cut the sample pieces manually.

Flexural characteristics of the composite boards exhibited a nearly linear increasing trend (Fig. 5). The highest bending strength (5.128 MPa) and the highest Young's modulus (3816.078 MPa) belong to the CEM5 panel, and the lowest values (1.038 MPa, 797.662 MPa, respectively) belong to CEM1. A nearly fivefold and steady rise is observed between the values of the two composite boards. It seems that the higher the amount of CM material in the mixture, the higher the flexural characteristics of the panels. One explanation may be that the elasticity values of raw reed materials are much weaker than those of coconut materials. This can be caused by the different chemical compositions between the lignocellulosic coir and reed materials. The other reason may be the slightly high sugar and tannin contents of the reed particles and the smooth long ribbed surface of the reed, which makes it difficult for the cement particles to contact the cellulosic materials. Due to the surface tension between the reed, the water droplet, and the law of surface friction, the water can easily move from the reed surface. It seems that the lignocellulosic coconut materials are more compatible with the cement than reed materials are. Another research study reported similar results for different cellulosic materials reinforced

Table 2
Regression analysis for flexural strength in terms of coir-reed materials compositions on different composites.

Effects	Flexural strength parameter	Flexural strength standard error	Flexural strength *T*	Flexural strength *p*
Intercept	−107.602	10.58303	−10.1674	0.000000
composition	1.076	0.10274	10.4765	0.000000

Table 3
Regression analysis for flexural modulus in terms of coir-reed materials compositions on different composites.

Effects	Young's Modulus parameter	Young's Modulus standard error	Young's Modulus *t*	Young's Modulus *p*
Intercept	−73704.2	9556.391	−7.71256	0.000003
Composition	741.7	92.772	7.99528	0.000002

Table 4
Regression analysis for internal bonding strength in terms of coir-reed materials compositions on different composites.

Effects	Internal Bonding strength parameter	Internal Bonding strength standard error	Internal Bonding strength *t*	Internal Bonding strength *p*
Intercept	−6.90833	0.549963	−12.5615	0.000000
Composition	0.06833	0.005339	12.7990	0.000000

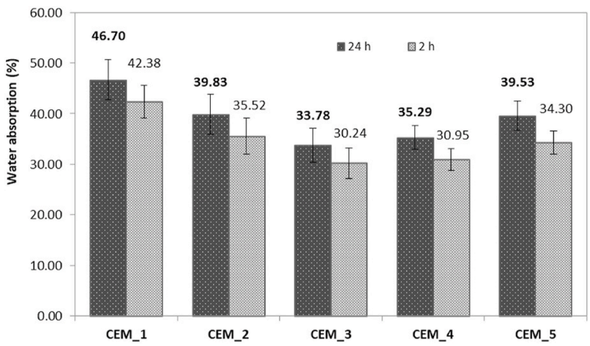

Fig. 7. Water absorption of composites.

composites [31].

Fig. 6 displays the mean values of internal bonding strengths of different composites. The diagram shows almost the same linear increase as in previous cases. CEM5 (0.31 MPa) exhibited the highest internal bonding strength, and CEM1 exhibited the lowest. As seen in the bending strength and Young's modulus investigations, the diagram reveals a weak connection between the individual reed materials and between the reed and the cement particles. The reasons are presumably the same. Other researchers have obtained similar results when mixing different lignocellulosic material-reinforced cementitious panels [45,46]. Consequently, the presence of reed degrades the flexural properties of composite boards, i.e., the higher the reed content, the weaker the boards. Table 2, Table 3, and Table 4 show the regression calculation. These results reflect a strong relationship between the groups, p-value remains below 0.05.

3.3. Physical properties investigation

Water absorption is one of the most significant factors in composite materials. Most problems in construction stem from capillary water uptake, which damages composites when exposed to moisture. Fig. 7 displays the water absorption values. Two effects occur simultaneously in this investigation. One is capillarity due to porosity, and the other is water binding due to the chemical structure of the raw materials. The reed-cement composite panel (CEM1) has the highest water absorption (46.70%), which can be caused by poor bonding between the reed and cement particles. Due to poor binding, the capillary absorption of water is significant because water molecules easily find their way into cavities. The chemical properties of the reeds can cause weak bonding. CEM3 panel (33.78%), in which the proportion of reed and coir is 50-50%, demonstrated the lowest water absorption. The values increase slightly from CEM3 to CEM5 (39.53%), where it almost reaches the value of CEM2. In the CEM5 panel, internal bonding strength and moisture content were the highest (0.31 MPa, 9.00%). This indicated that the bond between the fibrous materials did not weaken either despite the high-water content. The capillarity and water-binding are equally important for coir materials, and a stronger bond can be formed between the CM, RS and the cement particles. Other researchers have reported a similar outcome [12,47,48].

Thickness swelling is another important parameter for composites. In contrast to moisture content and other mechanical properties, the thickness swelling shows a continuous decrease from CEM1 to CEM5 as follows: 16.41; 9.19; 5.42; 4.29, and 3.68% (Fig. 8).

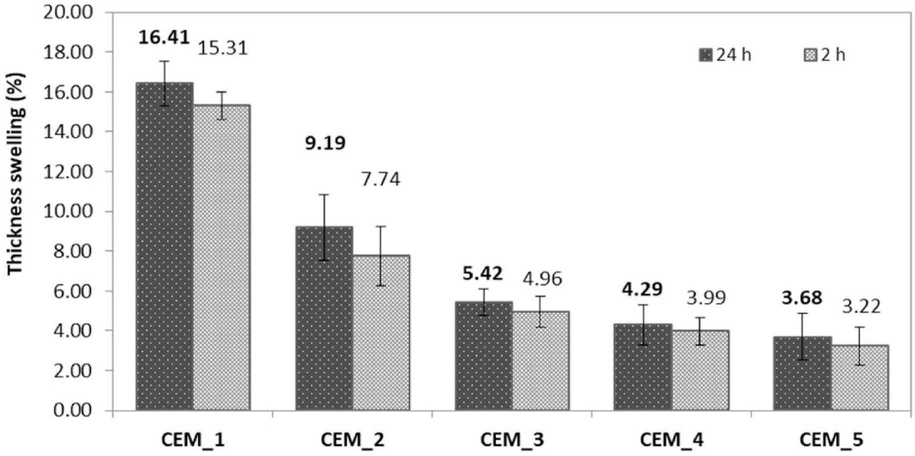

Fig. 8. Thickness swelling of composite boards.

Table 5
Regression analysis for moisture content in terms of coir-reed materials compositions on different composites.

Effects	Moisture Content parameter	Moisture Content standard error	Moisture Content *T*	Moisture Content *p*
Intercept	−59.8956	7.929719	−7.55331	0.000004
Composition	0.6591	0.076980	8.56236	0.000001

Table 6
Regression analysis for water absorption in terms of coir-reed materials compositions on different composites.

Effects	Water absorption parameter	Water absorption standard error	Water absorption *T*	Water absorption *p*
Intercept	253.9670	95.80879	2.65077	0.019982
Composition	−2.0898	0.93009	−2.24683	0.042656

Table 7
Regression analysis for thickness swelling in terms of coir-reed materials compositions on different composites.

Effects	Thickness swelling parameter	Thickness swelling standard error	Thickness swelling *t*	Thickness swelling *p*
Intercept	306.3032	43.89213	6.97854	0.000010
composition	−2.9017	0.42610	−6.81003	0.000012

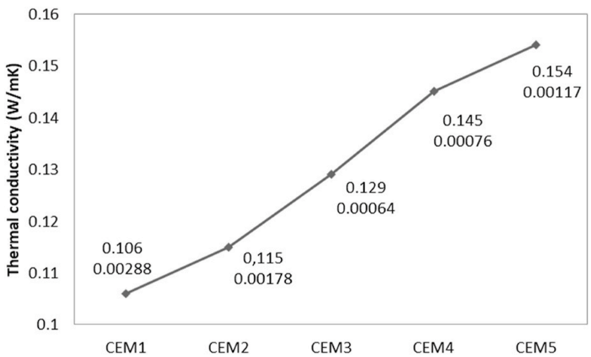

Fig. 9. Thermal conductivity of the composite boards.

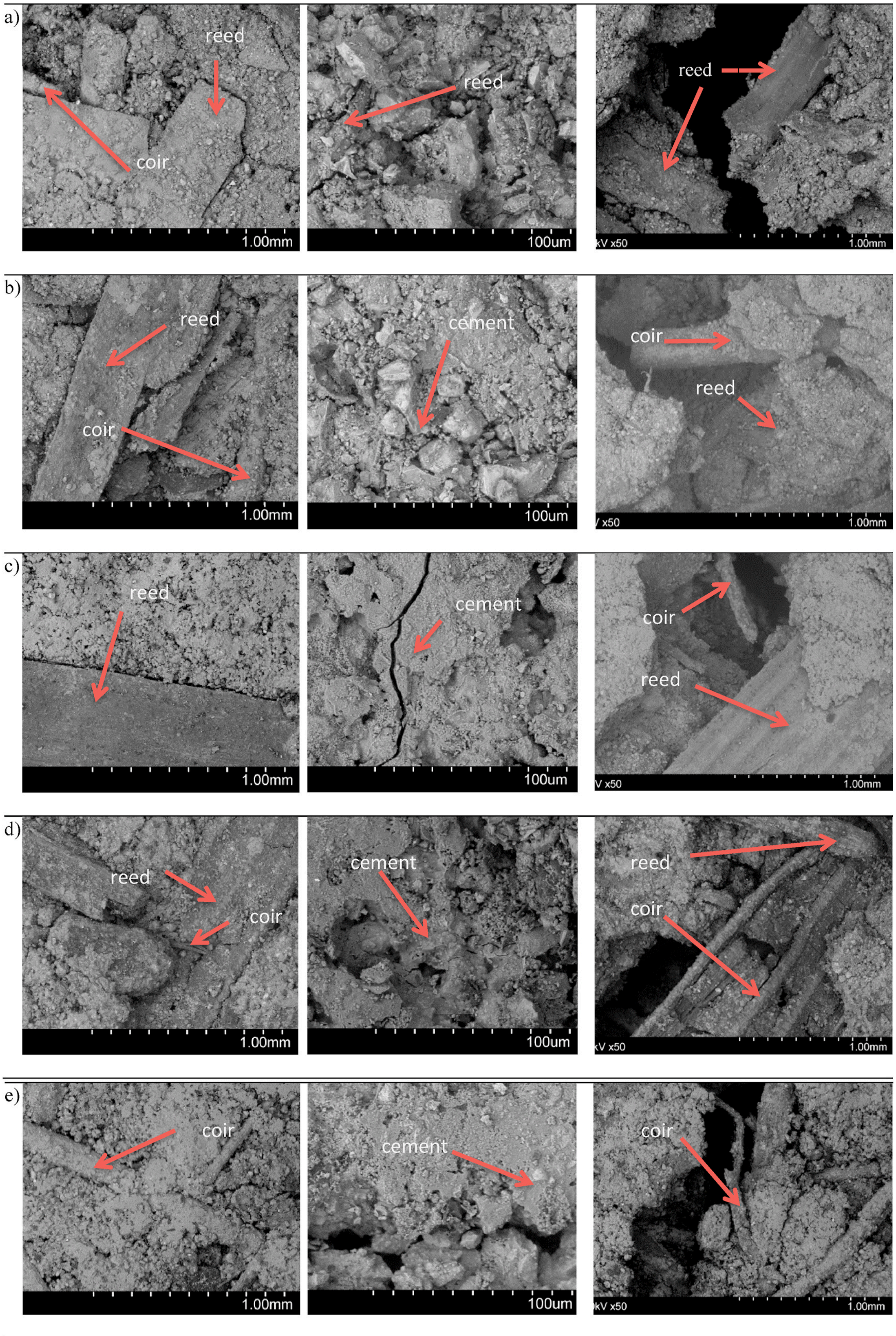

(caption on next page)

Fig. 10. SEM profiles zoom 50 left, zoom 500 middle; SEM micrographs of fractured zoom 50 right; a) CEM1; b) CEM2; c) CEM3; d) CEM4; e) CEM5.

Unsurprisingly, the weakest internally-bonded board had the highest thickness swelling, and the strongest board had the lowest thickness swelling. The figure reveals that the swelling appeared quickly and approached its final state [49] during the 2-h immersion [12,50]. Table 5, Table 6 and Table 7 show the regressive calculation of physical properties. The p-value remains below 0.05, indicating the strong comparability between the groups of the panels.

3.4. Thermal conductivity investigations

Thermal conductivity values of different composite panels were also investigated (Fig. 9) thermal conductivity of the finished composite boards were 0.106, 0.115, 0.129, 0.145, and 0.154 W/(m.K). By comparison, air has 0.026 W/(m.K), water has 0.6 W/(m.K), and cement stones have 1–3 W/(m.K). CEM1 has the lowest value, and CEM5 has the highest. Thermal conductivity values are between 0.10 and 0.15 W/(m.K); therefore, the difference was 0.05 W/(m.K), which is small. According to a multi-participant comprehensive study, the thermal conductivity of coir material is 0.58 W/(m.K). It seems the presence of coconut weakens the thermal insulation capacity of the boards. There is a relationship between the thermal conductivity and moisture content; however, the boards with more reed particle (CEM1) had better insulation quality, and a similar chart shape can be observed [31,51,52].

3.5. Morphological observation

SEM micrographs were investigated to assess the morphology of the developed products (Fig. 10). SEM pictures perfectly show the weak connection between the reed straw materials and the cement grains. The lamellar structure of the reed is visible, and its “clean” surface suggests that the cement grains could not be sufficiently bonded with it. Conversely, cement completely surrounds the thin coconut materials, which allows a strong bond between the two materials. Three panels (CEM2, CEM3, and CEM4) contain a mixture of reeds and coconut particles in different proportions. The images do not show any connection between the two threads. Due to its lamellar structure, the lignocellulosic particle portions of the reed must not mix with the coconut husk. As the right-hand column in Fig. 10 illustrates, a cracked surface appeared in the matrix. In the fractured parts, it is clear that the reeds were completely separated, but the fibrous coconut materials were difficult to dismantle. The discussions above also align with other studies [49].

3.6. EDX analysis

The examination of the elemental composition shows that the main components of the composite panels are O 45.43%, Ca 29.44%, C 13.6% and Si 6.52% (Fig. 11). The control study of the elemental composition of the raw materials confirms this result (Fig. 12). The predominant presence of O is observed in all three raw materials, with the presence of C in the case of coconut and reed (50.42 and 48.12%), and the presence of Ca in the case of cement (45.93%). In addition, all three raw materials contain small amounts of Si. Some other chemical elements like Mg, Al, Mo, Fe, K, and Na reflect a successful bonding of OPC and lignocellulosic coir and reed materials. The presence of C and O at different fragments was notable; interestingly, the presence of C is higher in coconut (50.42%) than in reed straw (48.12%). The coir and reed particles displayed the dominance of C and O in their polymeric structure, but this changed after the bonding with OPC for all five composite panels where the dominance of Si and Ca is also apparent due to the strong influence of OPC in the composite systems. The FTIR analysis further confirmed the bonding of the CM and RS with OPC.

3.7. FTIR analysis

Infrared spectroscopy determined the chemical interactions of each plate. The recorded infrared spectra ranged between 400 and 4000 cm^{-1} for this study. The FTIR study proves the existence of cellulosic materials in the produced composite panels (Fig. 13). The peaks at 2158–3700 cm^{-1} indicate the stretching vibrations of C–H and O–H bonds; the peaks within the 800–1600 cm^{-1} range are attributed to the cellulosic structure of natural cellulosic materials, and the peaks within 1104–1600 cm^{-1} correspond to the presence of hemicellulose and lignin. The crystalline area is observable around 1406 cm^{-1}, and the peaks at 868 cm^{-1} denote the amorphous region. The control reed and coir material show the presence of different chemical constituents of cellulose, hemicellulose, and lignin. The control cement highlights that the presence of cement greatly influenced the behaviour of the natural particles. This is most noticeable in boards with higher reed amounts (CEM1 − CEM3). The FTIR test further confirms a formed bond between the lignocellulosic materials and the cement. Similar discussions on FTIR also agree with some previous studies [31,53,54].

3.8. TGA/DTG analysis

Fig. 14 provides the thermal analysis of lignocellulosic coconut husk derived particles, reed straw particles, OPC materials, and their associated composites. The analysis indicates that cement is more thermally stable than coir and reed particles. In addition, coir is more stable than reeds. However, after the fabrication into composites, the thermal stability of the embedded products is enhanced. The primary weight loss at around 100 °C likely occurred due to moisture evaporation from the lignocellulosic reinforcements and OPC matrix. Moreover, the lignocellulosic materials displayed major weight loss from 250 to 430 °C, whereas their embedded products with OPC lost significant weight from 294 to 765 °C. The DTG analysis indicates that the thermal decompositions of CSH (hydrated calcium silicate) appear in the peaks between 80 and 165 °C. However, the peaks from 280 to 380 °C demonstrate the decomposition of lignocellulosic materials from the reinforcements and their products. The peaks within 385–476 °C correlate with $Ca(OH)_2$ dehydration [55]. Additionally, some minor peaks around 480 °C reflect the Portlandites decompositions. The phenomenon discussed here is also congruent with other cellulosic material/cement-based products [31,56].

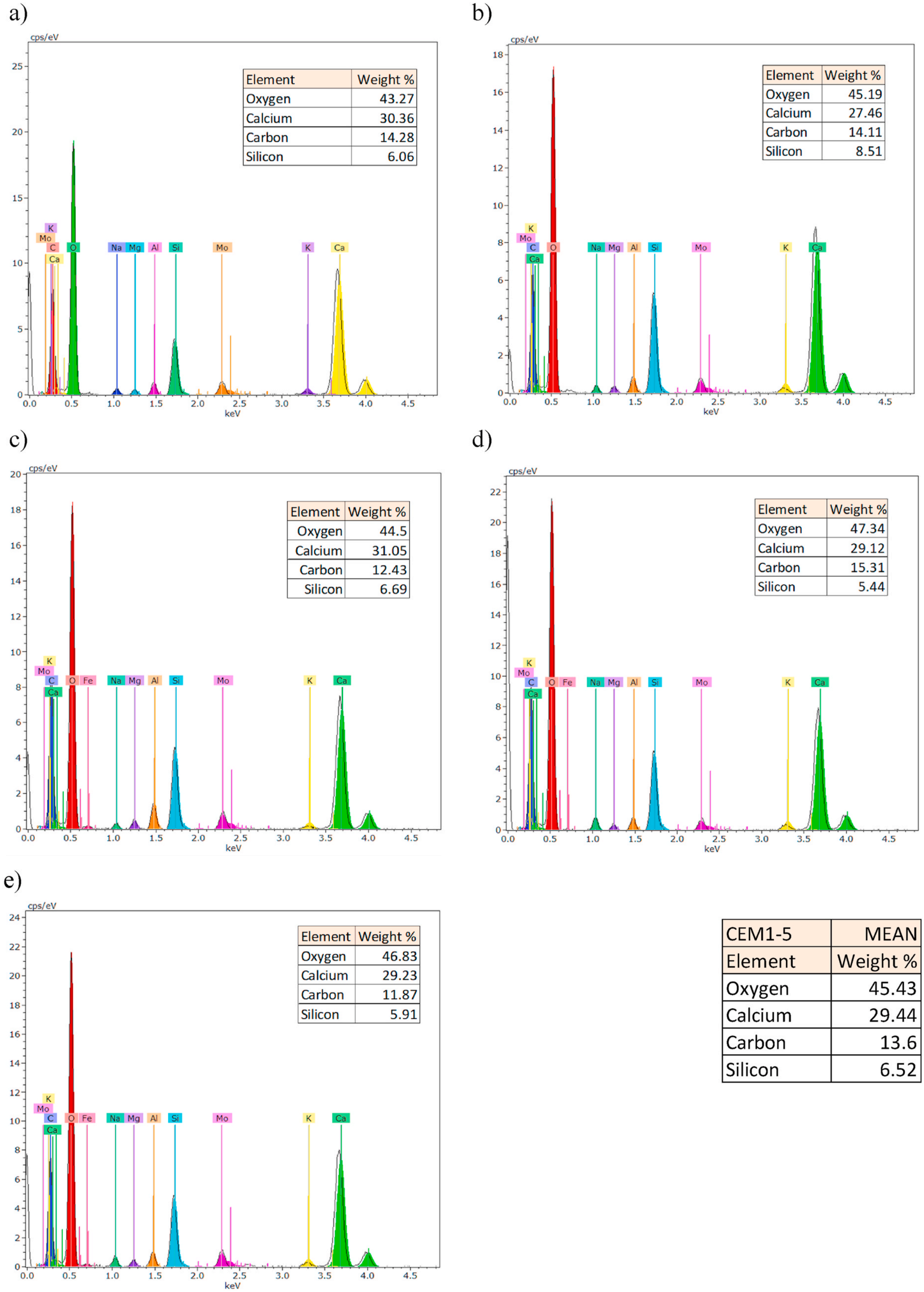

(caption on next page)

Fig. 11. EDX analysis; a) CEM1; b) CEM2; c) CEM3; d) CEM4; e) CEM5.

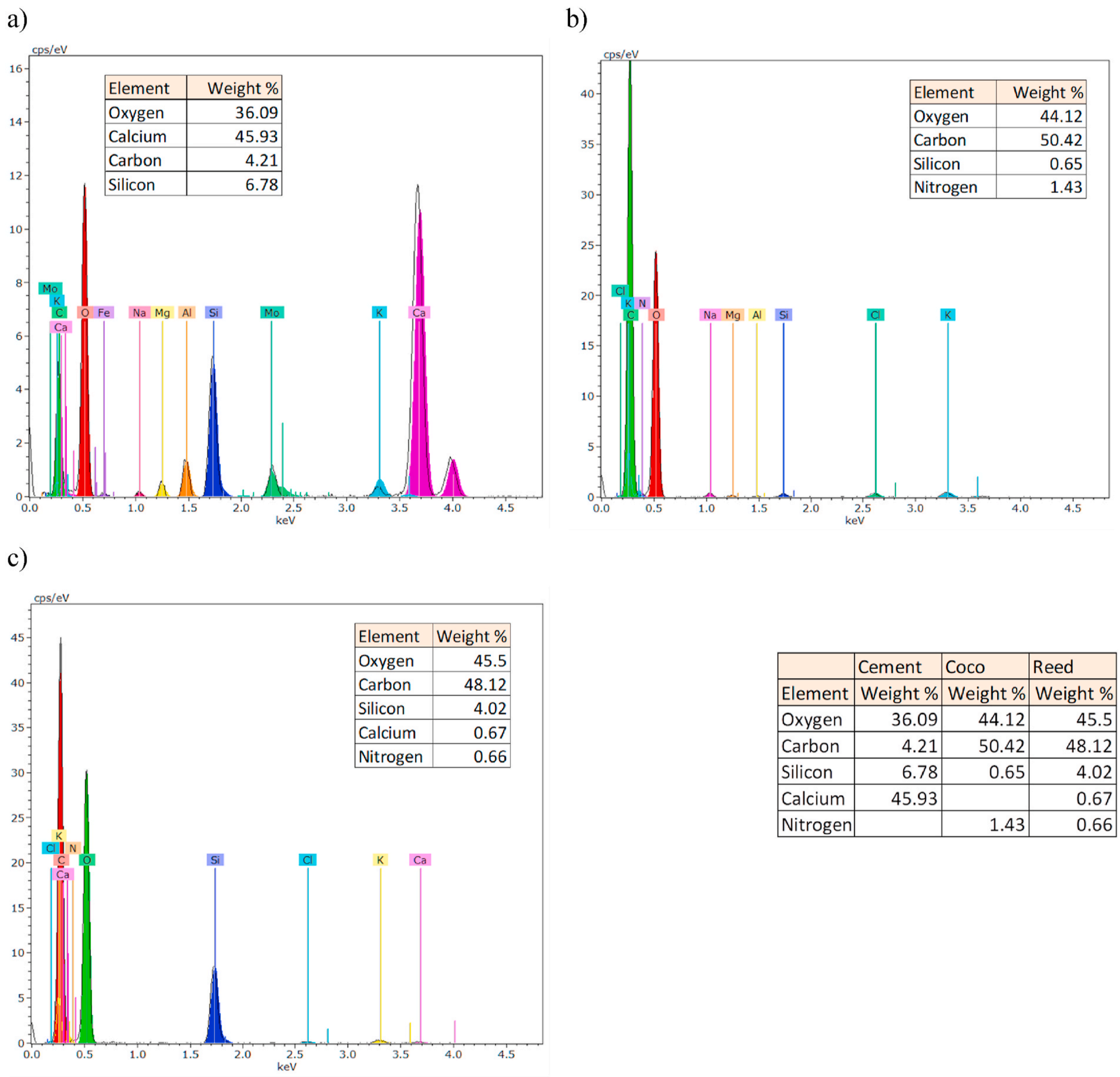

	Cement	Coco	Reed
Element	Weight %	Weight %	Weight %
Oxygen	36.09	44.12	45.5
Carbon	4.21	50.42	48.12
Silicon	6.78	0.65	4.02
Calcium	45.93		0.67
Nitrogen		1.43	0.66

Fig. 12. EDX analysis; a) cement control, b) coconut control, c) reed straw control.

4. Conclusions

The current study reported on a facile, innovative, and cost-efficient reinforcement of reed straw and coir materials by applying semi-dry technology in the presence of an OPC matrix. As reed and coir materials are naturally derived lignocellulosic materials, they offer tremendous potential for environmentally-friendly panel production. The results show that mechanical properties and the insulation performances exhibited an increasing trend with the increase in coir material in the panel constituents. The FTIR study confirmed the successful bonding between the lignocellulosic materials and the OPC matrix after the reinforcements. The fractured surfaces of panels also explicitly show the presence of energy reed and coir materials in the composites. The results obtained for physical tests of the samples also displayed better resistance against humid environments. The current study also noticed superior thermal stability, which increases with the increase of materials in the composite structure. Although this study established a reinforcement possibility among the reed and coir materials and OPC matrix, additional research on improving the mechanical properties of the insulation panels is still required. Overall, the mixture may be suitable for industrial use, primarily as an insulating or lightweight structure. However, the setting of the appropriate mixing ratio and technological processes needs further investigation.

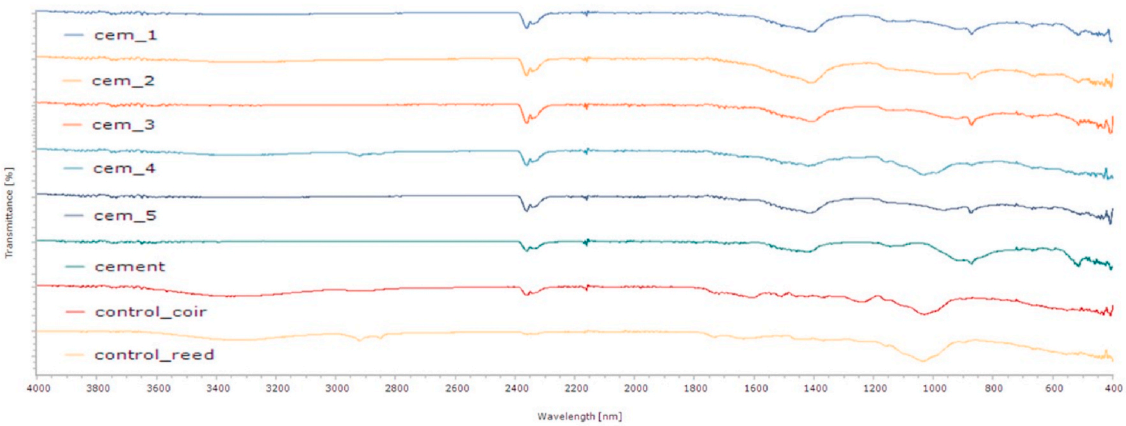

Fig. 13. FTIR spectra of cement composites (400-4000 cm^{-1}).

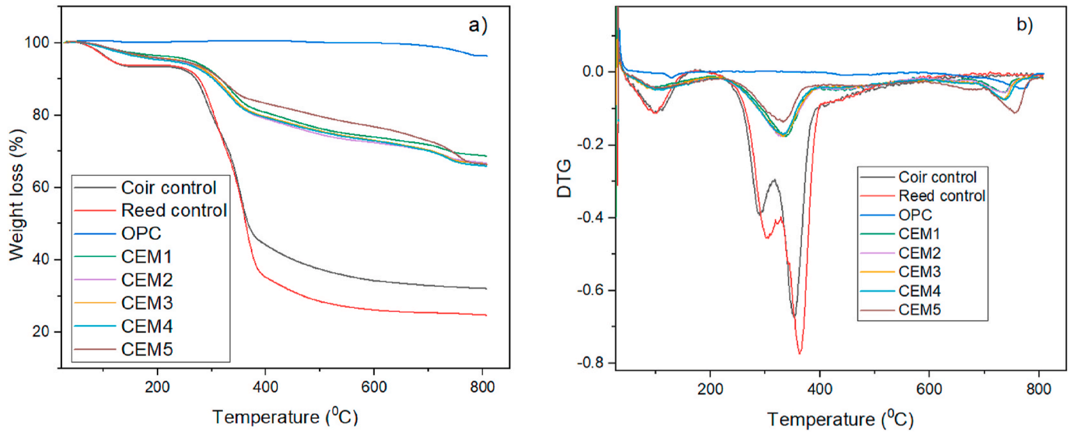

Fig. 14. TGA and DTG analysis of control coir and reed straw material and their reinforced OPC composites: a) TGA analysis and b) DTG analysis.

Author statement

Zsuzsanna Mária Mucsi: Writing - original draft, Writing - review and editing, Investigation, Methodology, Software, Visualization.**K. M. Faridul Hasan:** Writing - original draft, Writing - review & editing, Investigation, Methodology, Software, Visualization. **Péter György Horváth:** Writing - review & editing, Project administration, Resource, Validation, Data curation.**Miklós Bak:** Formal analysis, Methodology.**Zsófia Kóczán:** Formal analysis, Methodology.**Tibor Alpár:** Writing - review & editing, Project administration, Resource, Validation, Data curation.

Declaration of competing interest

The authors declare that they have no known competing financial interests or personal relationships that could have appeared to influence the work reported in this paper.

Acknowledgments

This work was supported by the “Stipendium Hungaricum” scholarship under the Faculty of Wood Engineering and Creative Industries at the University of Sopron, Hungary. This article was produced within the framework of “TKP2021-NKTA-43” project with the support provided by the Ministry of Innovation and Technology of Hungary from the National Research, Development and Innovation Fund, financed under the TKP2021-NKTA funding scheme. Authors are also grateful to Kun Gábor and Tamás Hofmann (University of Sopron) for their cooperation in this research.

References

[1] H. Dahy, Biocomposite materials based on annual natural fibres and biopolymers – design, fabrication and customized applications in architecture, Construct. Build. Mater. 147 (2017) 212–220, https://doi.org/10.1016/j.conbuildmat.2017.04.079.

[2] P. Cao, X. Guo, R. Li, Architectural (decorative) natural fiber composites for construction, in: M. Fan, F. Fu (Eds.), Advanced High Strength Natural Fibre Composites in Construction, Elsevier, Duxford, United Kingdom, 2017, pp. 425–445.
[3] M. Fan, Future scope and intelligence of natural fibre based construction composites, in: M. Fan, F. Fu (Eds.), Advanced High Strength Natural Fibre Composites in Construction, Elsevier, London, United Kingdom, 2017, pp. 545–556.
[4] N. Saba, et al., Green biocomposites for structural applications, in: M. Jawaid, M.S. Salit, O.Y. Alothman (Eds.), Green Biocomposites, Springer, Cham, 2017, pp. 1–27.
[5] A. Mohanty, M.a. Misra, G. Hinrichsen, Biofibres, biodegradable polymers and biocomposites: an overview, Macromol. Mater. Eng. 276 (2000) 1–24.
[6] M. Yildirim, et al., Development and characterization of hybrid composites from sustainable green materials, Green Mater. 9 (2020) 182–191.
[7] A. Merzoug, et al., Quasi-static and dynamic mechanical thermal performance of date palm/glass fiber hybrid composites, J. Ind. Textil. (2020), 1528083720958036.
[8] S. Mahmud, et al., Comprehensive review on plant fiber-reinforced polymeric biocomposites, J. Mater. Sci. 56 (2021) 7231–7264, https://doi.org/10.1007/s10853-021-05774-9.
[9] K. Kochova, et al., Using alternative waste coir fibres as a reinforcement in cement-fibre composites, Construct. Build. Mater. 231 (2020), 117121, https://doi.org/10.1016/j.conbuildmat.2019.117121.
[10] T. Cardinale, et al., Investigations on thermal and mechanical properties of cement mortar with reed and straw fibers, Int. J. Heat Technol. 35 (2017) S375–S382, https://doi.org/10.18280/ijht.35Sp0151.
[11] N. Ayrilmis, et al., Effect of boron and phosphate compounds on physical, mechanical, and fire properties of wood–polypropylene composites, Construct. Build. Mater. 33 (2012) 63–69.
[12] K.F. Hasan, P.G. Horváth, T. Alpár, Development of lignocellulosic fiber reinforced cement composite panels using semi-dry technology, Cellulose 28 (2021) 3631–3645, https://doi.org/10.1007/s10570-021-03755-4.
[13] K.F. Hasan, et al., A state-of-the-art review on coir fiber-reinforced biocomposites, RSC Adv. 11 (2021) 10548–10571, https://doi.org/10.1039/D1RA00231G.
[14] D. Nath Barman, et al., Effect of mild alkali pretreatment on structural changes of reed (Phragmites communis Trinius) straw, Environ. Technol. 35 (2014) 232–241, https://doi.org/10.1080/09593330.2013.824009.
[15] T. Hamouda, et al., Evaluation of mechanical and physical properties of hybrid composites from food packaging and textiles wastes, J. Polym. Environ. 27 (2019) 489–497.
[16] K.F. Hasan, et al., Rice straw and energy reed fibers reinforced phenol formaldehyde resin polymeric biocomposites, Cellulose 28 (2021) 7859–7875, https://doi.org/10.1007/s10570-021-04029-9.
[17] K. Hasan, P.G. Horváth, T. Alpár, Potential natural fiber polymeric nanobiocomposites: a review, Polymers 12 (2020) 1072, https://doi.org/10.3390/polym12051072.
[18] A.H. Hassanin, et al., Developing high-performance hybrid green composites, Compos. B Eng. 92 (2016) 384–394.
[19] E. Avci, et al., Manufacturing biocomposites using black pine bark and oak bark, Bioresources 13 (2018) 15–26.
[20] K.F. Hasan, et al., Enhancing mechanical and antibacterial performances of organic cotton materials with greenly synthesized colored silver nanoparticles, Int. J. Cloth. Sci. Technol. (2022), https://doi.org/10.1108/IJCST-05-2021-0071.
[21] K. Hasan, et al., Colorful and facile in situ nanosilver coating on sisal/cotton interwoven fabrics mediated from European larch heartwood, Sci. Rep. 11 (2021) 1–13, https://doi.org/10.1038/s41598-021-01914-y.
[22] K.M.F. Hasan, P.G. Horváth, T. Alpár, Effects of Alkaline Treatments on Coconut Fiber Reinforced Biocomposites in 9th Interdisciplinary Doctoral Conference, Doctoral Student Association of the University of Pécs, Pecs, Hungary, 2020.
[23] K. Hasan, et al., Novel insulation panels development from multilayered coir short and long fiber reinforced phenol formaldehyde polymeric biocomposites, J. Polym. Res. 28 (2021) 1–16, https://doi.org/10.1007/s10965-021-02818-1.
[24] V.K. Singh S. Mukhopadhyay, Studies on the effect of hybridization on sound insulation of coir-banana-polypropylene hybrid biocomposites, J. Nat. Fibers (2020) 1–10, https://doi.org/10.1080/15440478.2020.1745116.
[25] K. Hasan, et al., Novel insulation panels development from multilayered coir short and long fiber reinforced phenol formaldehyde polymeric biocomposites, J. Polym. Res. 28 (2021) 1–16, https://doi.org/10.1007/s10965-021-02818-1.
[26] C. Asasutjarit, et al., Development of coconut coir-based lightweight cement board, Construct. Build. Mater. 21 (2007) 277–288, https://doi.org/10.1016/j.conbuildmat.2005.08.028.
[27] N. Md Sadiqu, et al., The use of coconut fibre in the production of structural lightweight concrete, Res. J. Appl. Sci. 12 (2012) 831–839, https://doi.org/10.3923/jas.2012.831.839.
[28] A.I. Engloner, Structure, growth dynamics and biomass of reed (Phragmites australis)–A review, Flora, Morphol. Distrib. Funct. Ecol. Plants 204 (2009) 331–346, https://doi.org/10.1016/j.flora.2008.05.001.
[29] R. Pude, et al., Suitability of Phragmites for lightweight concrete, J. Appl. Bot. Food Qual. 79 (2005) 141.
[30] J. Khedari, et al., New low-cost insulation particleboards from mixture of durian peel and coconut coir, Build. Environ. 39 (2004) 59–65, https://doi.org/10.1016/j.buildenv.2003.08.001.
[31] K.F. Hasan, et al., Semi-dry technology-mediated coir fiber and Scots pine particle-reinforced sustainable cementitious composite panels, Construct. Build. Mater. 305 (2021), 124816, https://doi.org/10.1016/j.conbuildmat.2021.124816.
[32] E. Avci, Z. Candan, O. Gonultas, Performance properties of biocomposites from renewable natural resource, J. Compos. Mater. 48 (2014) 3237–3242.
[33] K.F. Hasan, et al., Design and fabrication technology in biocomposites manufacturing, in: M. Sriariyanun, et al. (Eds.), Value-added Biocomposites: Technology, Innovation, and Opportunity, CRC Press, Boca Raton, USA, 2021, pp. 158–183.
[34] K.F. Hasan, P.t.G.r. Horváth, T. Alpár, Nanotechnology for waste wood recycling, in: Nanotechnology in Paper and Wood Engineering, Woodhead Publishing, Duxford, United Kingdom, 2022, pp. 61–80.
[35] K.M.F. Hasan, P.G. Horváth, T. Alpár, Lignocellulosic fiber cement compatibility: a state of the art review, J. Nat. Fibers (2021) 1–26, https://doi.org/10.1080/15440478.2021.1875380.
[36] K. Hasan, et al. Effects of cement on lignocellulosic fibres. in 9th Hardwood Proceedings. 2020. Sopron, Hungary: University of Sopron Press.
[37] M. Ali, Coconut fibre: a versatile material and its applications in engineering, J. Civ. Eng. 2 (2011) 189–197, https://doi.org/10.5897/JCECT.9000009.
[38] V. Mathur, Composite materials from local resources, Construct. Build. Mater. 20 (2006) 470–477, https://doi.org/10.1016/j.conbuildmat.2005.01.031.
[39] L.A. Tibor, G.H. Péter, K.M.F. Hasan, Introduction to biomass and biocomposites, in: Toward the Value-Added Biocomposites: Technology, Innovation and Opportunity, CRC Press, Boca Raton, USA, 2021.
[40] A. Akhavan, J. Catchmark, F. Rajabipour, Ductility enhancement of autoclaved cellulose fiber reinforced cement boards manufactured using a laboratory method simulating the Hatschek process, Construct. Build. Mater. 135 (2017) 251–259, https://doi.org/10.1016/j.conbuildmat.2017.01.001.
[41] A. Moslemi, Emerging technologies in mineral-bonded wood and fiber composites, Adv. Perform. Mater. 6 (1999) 161–179, https://doi.org/10.1023/A:1008777812842.
[42] V. Ezerskiy, N.V. Kuznetsova, A.D. Seleznev, Evaluation of the use of the CBPB production waste products for cement composites, Construct. Build. Mater. 190 (2018) 1117–1123, https://doi.org/10.1016/j.conbuildmat.2018.09.148.
[43] R. Malkapuram, V. Kumar, Y.S. Negi, Recent development in natural fiber reinforced polypropylene composites, J. Reinforc. Plast. Compos. 28 (2009) 1169–1189.
[44] S. Ferreiro, D. Herfort, J. Damtoft, Effect of raw clay type, fineness, water-to-cement ratio and fly ash addition on workability and strength performance of calcined clay–limestone Portland cements, Cement Concr. Res. 101 (2017) 1–12, https://doi.org/10.1016/j.cemconres.2017.08.003.
[45] P. Lertwattanaruk A. Suntijitto, Properties of natural fiber cement materials containing coconut coir and oil palm fibers for residential building applications, Construct. Build. Mater. 94 (2015) 664–669, https://doi.org/10.1016/j.conbuildmat.2015.07.154.

[46] L. Yan, et al., Effect of alkali treatment on microstructure and mechanical properties of coir fibres, coir fibre reinforced-polymer composites and reinforced-cementitious composites, Construct. Build. Mater. 112 (2016) 168–182, https://doi.org/10.1016/j.conbuildmat.2016.02.182.
[47] J. Wei, C. Meyer, Degradation mechanisms of natural fiber in the matrix of cement composites, Cement Concr. Res. 73 (2015) 1–16, https://doi.org/10.1016/j.cemconres.2015.02.019.
[48] T. Hamouda, et al., Hybrid composites from coir fibers reinforced with woven glass fabrics: physical and mechanical evaluation, Polym. Compos. 38 (2017) 2212–2220.
[49] P. He, C.S. Poon, D.C. Tsang, Water resistance of magnesium oxychloride cement wood board with the incorporation of supplementary cementitious materials, Construct. Build. Mater. 255 (2020), 119145, https://doi.org/10.1016/j.conbuildmat.2020.119145.
[50] L. Aggarwal, et al., Cement-bonded composite boards with arhar stalks, Cem. Concr. Compos. 30 (2008) 44–51, https://doi.org/10.1016/j.cemconcomp.2007.07.004.
[51] A.H. Hassanin, et al., Thermal insulation properties of hybrid textile reinforced biocomposites from food packaging waste, J. Ind. Textil. 47 (2018) 1024–1037.
[52] H. Zhang, et al., Dynamic thermal performance of ultra-light and thermal-insulative aerogel foamed concrete for building energy efficiency, Sol. Energy 204 (2020) 569–576.
[53] M. Ghofrani, et al., Fiber-cement composite using rice stalk fiber and rice husk ash: mechanical and physical properties, J. Compos. Mater. 49 (2015) 3317–3322. https://doi.org/10.1177/0021998314561813.
[54] A. Ashori, T. Tabarsa, S. Sepahvand, Cement-bonded composite boards made from poplar strands, Construct. Build. Mater. 26 (2012) 131–134, https://doi.org/10.1016/j.conbuildmat.2011.06.001.
[55] P.R. Lima, et al., Deflection hardening of sustainable fiber–cement composites, Green Mater. 4 (2016) 18–30, https://doi.org/10.1680/jgrma.15.00018.
[56] M.R. Cabral, et al., Evaluation of accelerated carbonation curing in cement-bonded balsa particleboard, Mater. Struct. 51 (2018) 52, https://doi.org/10.1617/s11527-018-1179-y.